Final Report for AOARD Grant **FA2386-09-1-4092**

Photophysical Properties on Möbius Aromatic and Antiaromatic Expanded Porphyrins

20th, September 2010

Principal Investigators: Prof. Dongho Kim

E-mail address: dongho@yonsei.ac.kr

Institution: Spectroscopy Laboratory for Functional π-electronic Systems and Department of Chemistry, Yonsei University, Seoul 120-749, Korea

Mailing Address: 134 Shinchon-dong, Seodaemun-gu, Seoul 120-749, Korea

Phone: +82-2-2123-2436

Fax: +82-2-2123-2434

Period of Performance: 16/05/2009 – 15/05/2010

Report Documentation Page

Form Approved
OMB No. 0704-0188

1. REPORT DATE	2. REPORT TYPE	3. DATES COVERED
22 SEP 2010	**FInal**	**14-04-2009 to 20-09-2010**

4. TITLE AND SUBTITLE
Photophysical Properties on Mobius and Antiaromatic Expanded Porphyrins

5a. CONTRACT NUMBER
FA23860914092

5b. GRANT NUMBER

5c. PROGRAM ELEMENT NUMBER

6. AUTHOR(S)
Dongho Kim

5d. PROJECT NUMBER

5e. TASK NUMBER

5f. WORK UNIT NUMBER

7. PERFORMING ORGANIZATION NAME(S) AND ADDRESS(ES)
Yonsei University,Shinchon-Dong 134, Seodaemoon-Ku,Seoul 120-749,Korea (South),KR,120-749

8. PERFORMING ORGANIZATION REPORT NUMBER
N/A

9. SPONSORING/MONITORING AGENCY NAME(S) AND ADDRESS(ES)
AOARD, UNIT 45002, APO, AP, 96337-5002

10. SPONSOR/MONITOR'S ACRONYM(S)
AOARD

11. SPONSOR/MONITOR'S REPORT NUMBER(S)
AOARD-094092

12. DISTRIBUTION/AVAILABILITY STATEMENT
Approved for public release; distribution unlimited

13. SUPPLEMENTARY NOTES

14. ABSTRACT
Expanded porphyrins have come to the forefront in the research field of aromaticity and been recognized as the most appropriate molecular system to study M?bius aromaticity because their molecular topologies can be easily changed and controlled by various methods. Along with this advantage, many efforts have been devoted to the exploration of aromaticity-molecular topology relationship based on electronic structures in expanded porphyrins so that further insight into the aromaticity, very attractive term for chemists, can be provided. In this report, we have investigated the recent progresses of various M?bius (anti)aromatic expanded porphyrins and their photophysical properties in conjunction with the topological transformation between H?ckel and M?bius aromaticity by various conformational control methods, such as ring fusion and protonation.

15. SUBJECT TERMS
Materials Characterization, Materials Chemistry, Nonlinear Optical Materials, Spectroscopy

16. SECURITY CLASSIFICATION OF:			17. LIMITATION OF ABSTRACT	18. NUMBER OF PAGES	19a. NAME OF RESPONSIBLE PERSON
a. REPORT	b. ABSTRACT	c. THIS PAGE			
unclassified	**unclassified**	**unclassified**	**Same as Report (SAR)**	**24**	

Table of Contents

1. Abstract

Recently, expanded porphyrins have come to the forefront in the research field of aromaticity and been recognized as the most appropriate molecular system to study Möbius aromaticity because their molecular topologies can be easily changed and controlled by various methods. Along with this advantage, many efforts have been devoted to the exploration of aromaticity-molecular topology relationship based on electronic structures in expanded porphyrins so that further insight into the aromaticity, very attractive term for chemists, can be provided. In this report for *AFSOR/AOARD project* (***FA2386-09-1-4092***), we have investigated the recent progresses of various Möbius (anti)aromatic expanded porphyrins and their photophysical properties in conjunction with the topological transformation between Hückel and Möbius aromaticity by various conformational control methods such as ring fusion and protonation etc.

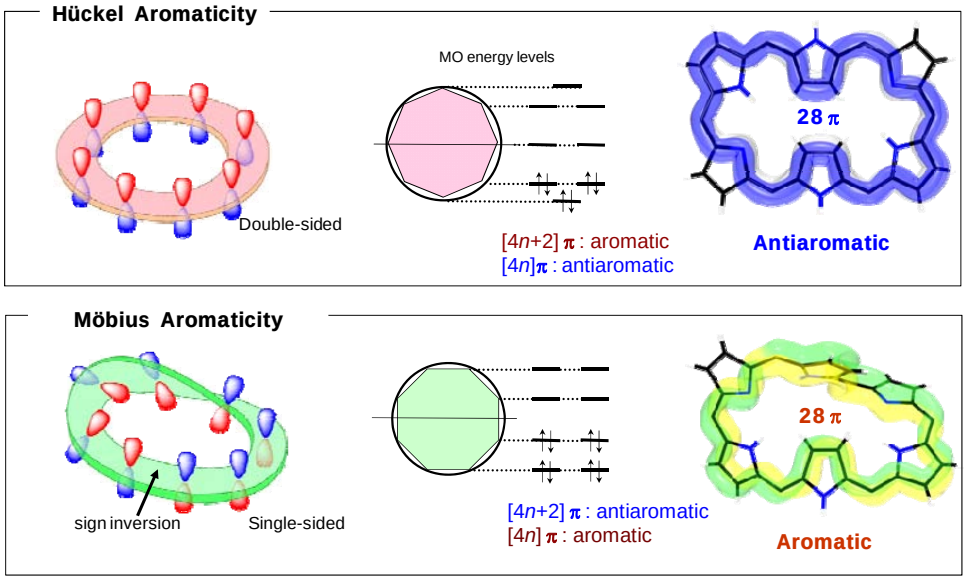

2. Introduction

Recently, expanded porphyrins containing more than four pyrrole rings have emerged as a promising class of molecules for applications in near-infrared (NIR) dyes, anion sensors, nonlinear optical (NLO) materials, photosensitizers and photodynamic therapy, due to their extended cavity sizes with larger number of π-electrons (Chart 1).

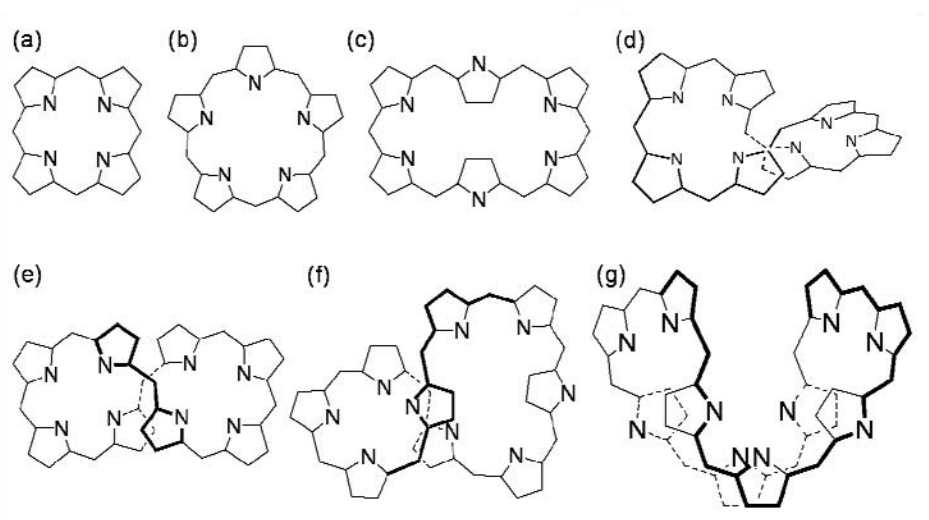

Chart 1 Various structures of porphyrinoids.

Owing to their extended π-conjugation pathways compared to tetrapyrrolic macrocycles, expanded porphyrins exhibit continuously red-shifted absorption bands, as the size of macrocycles increases (**Fig. 1**). Numerous kinds of expanded porphyrin have hitherto been prepared due to their, in principle, facile synthetic modifications by inserting heavy metals (i.e. Zn, Pd and Pt etc.), connecting the pyrrole rings, changing substituents in *meso*- and *β*-carbons and replacing the pyrrole rings with thiophene or furan rings, and so on. Among numerous kinds of expanded porphyrins, penta- and hexapyrrolic expanded porphyrins exhibit nearly planar structures due to their relatively small cavity sizes. On the other hand, as the number of pyrrole rings is larger than six, the overall molecular structures reveal distorted figure eight topologies. Thus, while the absorption bands of representative planar expanded porphyrin series show the continuous red-shifts (**Fig. 1**), some of larger expanded porphyrins which contain more than 6 pyrrole rings with distorted figure eight topologies exhibit broad and ill-defined absorption spectra. Since the overall molecular structures of expanded porphyrins largely determine the electronic structures through their π-conjugation

pathways, it is relevant to control the molecular topologies for better understanding of the structure/property relationship in expanded porphyrins. In this regard, various attempts to modify the overall structures of expanded porphyrins have been made by metal coordination, temperature, protonation with appropriate acids and functional group modifications. With these active modification methods of molecular topologies in hand, the electronic structures of expanded porphyrins have been explored by various spectroscopic measurements as well as theoretical calculations.

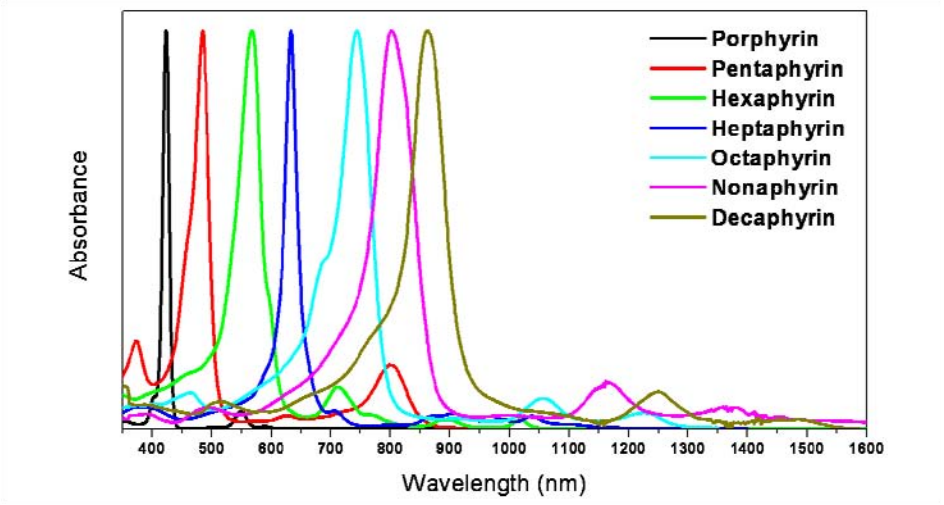

Fig. 1. Steady-state absorption spectra of expanded porphyrins.

In this final report (*AFSOR/AOARD project (**FA2386-09-1-4092**)*, we have described our observations of photophysical properties in several expanded porphyrins related with Möbius aromaticity on the basis of results attained by various time-resolved spectroscopic techniques, femtosecond Z-scan measurements, and quantum mechanical calculations.

3. Experimental Details

(1) Experimental Method

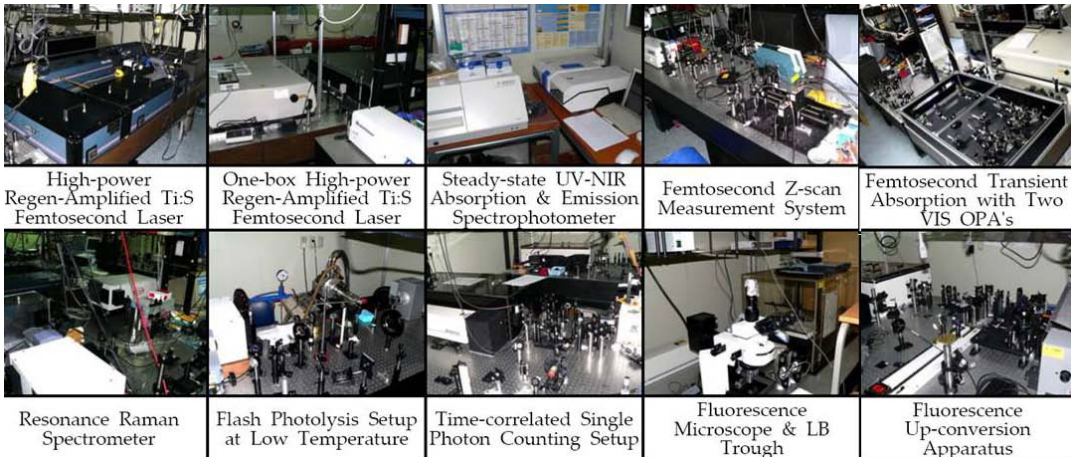

① **Steady-state Laser Spectroscopy**

- Laser-induced Luminescence Spectroscopy
- Resonance Raman Spectroscopy

② **Time-resolved Laser Spectroscopy**

- Nanosecond Flash Photolysis
- Picosecond Time-correlated Single Photon Counting (TCSPC) Method
- Vis/IR Femtosecond Transient Absorption Spectroscopy
- Femtosecond Fluorescence Up-conversion Spectroscopy

③ **Non-linear Spectroscopy**

- Femtosecond Z-scan Method

(2) Quantum Mechanical Calculation

- Nuclear-Independent Chemical Shift (**NICS**) Values
- Anisotropy of the Induced Current Density (**AICD**) Calculation
- Molecular Orbitals & Electronic Excited-state Excitation Energies

4. Results and Discussion

(1) Realization of Möbius aromatic molecules through ring fusion

The new developed method for the realization of Möbius aromatic expanded porphyrin is to use ring fusion reaction. By the fusion of two or more rings in a proper manner, both the rigid and flexible parts can coexist in one molecule at the same time, which is known as a critical factor for synthesizing the molecule with Möbius topology. The ring fusion reaction is paid much attention of chemists because it allows us to investigate thoroughly the intrinsic properties of Möbius aromatic expanded porphyrins without any interference such as metalation and protonation that can affect the photophysical properties in general. The two Möbius aromatic molecules tailored by this method have been reported so far – benzopyrane-fused [28]hexaphyrin **1** and thienyl-fused [28]hexaphyrin **2** (Chart 2).

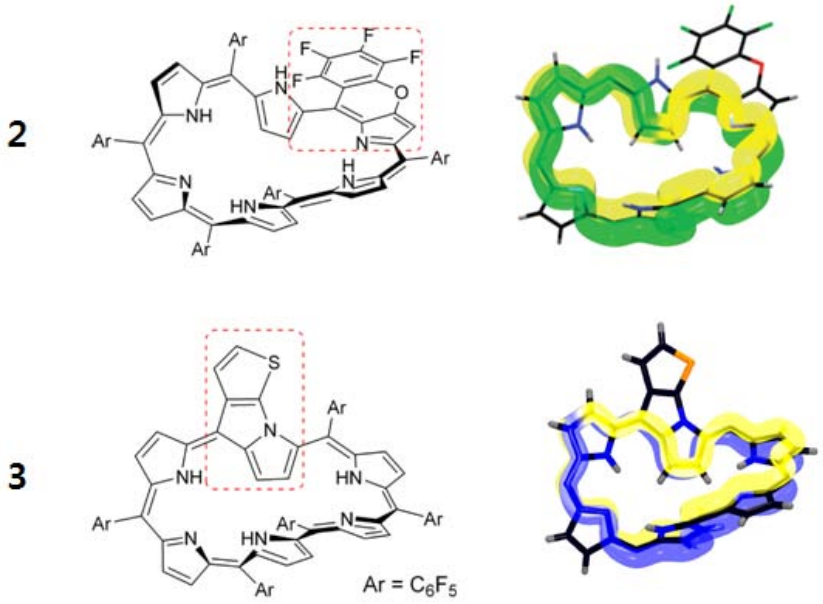

Chart 2. Schematic molecular structures and π-electron conjugation pathways of benzopyrane-fused [28]hexaphyrin **1** and thienyl-fused [28]hexaphyrin **2**

① Aromaticity and Photophysical Properties of Benzopyrane-fused [28]Hexaphyrins

In benzopyrane-fused [28]hexaphyrin **1**, pentafluorophenyl group at one of the *meso* positions is bound to the *β*-position of neighboring pyrrole through an oxygen atom (**Chart 2**). This fused geometry provides the twisted framework of Möbius topology, even at room temperature. The ^{1}H NMR spectrum of benzopyrane-fused [28]hexaphyrin **1** exhibits a distinct diatropic ring current. The peaks of two inner *β*-pyrrolic protons appear in shielded region (δ = -1.03 and 2.22 ppm), while those of outer *β*-pyrrolic protons are in deshielded

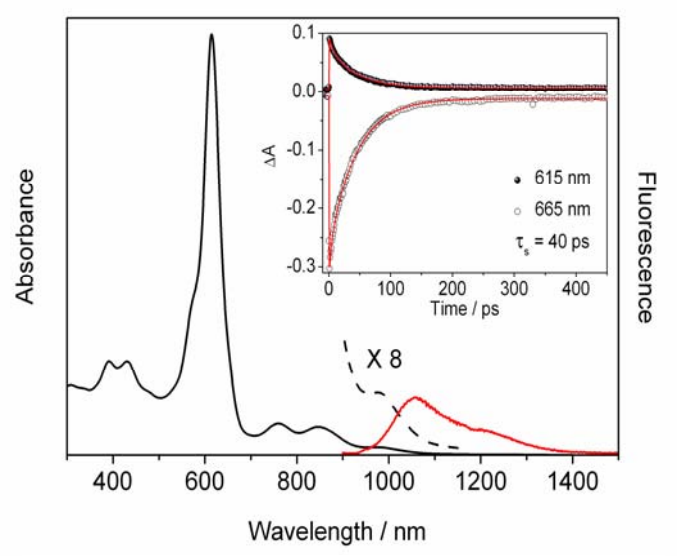

Fig. 2 Steady-state absorption (black line) and fluorescence (red line) spectra, and femtosecond transient absorption decay profiles (inset) of **1**.

region (δ = 5.45 ~ 7.44 ppm). Furthermore, the HOMA value was estimated to be 0.73 and the NICS value was evaluated to be -11.8 ppm at the central position of the molecule, suggesting the aromatic character of **1**.

The steady-state absorption spectrum of **1** exhibits typical characteristics of aromatic expanded porphyrins (**Fig. 2**). It shows an intense and sharp B-like band at 613 nm with a weak shoulder, two distinct Q-like bands at 760 and 844 nm, and one smeared Q-like band at 968 nm. In addition, the broad fluorescence spectra were observed at 1058 nm with large Stokes shift (879 cm^{-1}), indicating significant structural changes in the excited-state. Indeed, the excited-state dynamics reflects its structural flexibility. The singlet excited-state lifetime of **1** (ca. 40 ps at Room Temp.) is relatively short as compared to those of other aromatic hexaphyrins. This means that the aromatic stabilization effects are not strong enough to compensate the molecular flexibility given by its twisted molecular framework. Furthermore, the triplet excited-state dynamics was not detected at room temperature, but at 173 K the triplet excited-state lifetime was determined to be 350 ns. This temperature dependent triplet excited-state dynamics demonstrates that the conformational flexibility seems to play a crucial role in the excited-state depopulation process because at low temperature the flexible motions which can accelerate the nonradiative decay processes are limited. In addition, **1** has fairly large TPA cross-section ($\sigma^{(2)}$) value of 5400 GM, reflecting its efficient π-delocalization. When we compare qualitatively the experimental parameters (Δδ or $\sigma^{(2)}$) of **1** with other Möbius aromatic hexaphyrins, it can be noticed that the degree of π-delocalization in **1** is smaller than that of Möbius aromatic conformer in free-base [28]hexaphyrin at low temperature but similar to those of Möbius aromatic metalated [28]hexaphyrins. This may be attributed to the dihedral angles in the π-conjugation pathway determined by topology control, which affects how smoothly p-orbitals are overlapped with each other.

② Aromaticity and Photophysical Properties of Thienyl-fused [28]Hexaphyrins

As a successive work of synthesizing Möbius aromatic expanded porphyrins by ring fusion, thienyl-fused [28]hexaphyrin **2** has been reported. To begin with, spectacles-like shaped 5,20-bis(3-thienyl)-10,15,25,30-tetrakis(pentafluorophenyl)-substituted [26]hexaphyrin was used to produce Möbius aromatic hexaphyrin with an aid of the former study. However, this type of hexaphyrin having two thienly substituents turned out to be ineffective for our purpose because the reaction results in the mixture of two different hexaphyrins – doubly spiro-annulated [26]hexaphyrin and singly thienyl-fused [28]hexaphyrin. To make things even worse, the latter one has another spectacles-like planar conformer, namely Hückel antiaromatic [28]hexaphyrin, at room temperature even though its major isomer substantially shows Möbius aromatic character. To improve the yields, mono(3-thienyl)-pentakis(pentafluorophenyl) [26]hexaphyrin was introduced by substituting one 3-thienyl group for a large pentafluorophenly group as a reactant since there is no possibility to form the doubly spiro-annulated hexaphyrin. This rectangular-like shaped [26]hexaphyrin quantitatively gave thienyl-fused [28]hexaphyrin **2** by thermal fusion reaction. There is also the conformational dynamics between two Möbius aromatic enantiomers each other, and between them and Hückel antiaromatic conformer, but the contribution of Hückel antiaromatic one is negligible at room temperature. As a result, the strong diatropic ring current appears in its ^{1}H NMR spectra. Particularly, the difference in chemical shift between the inner and outer protons ($\Delta\delta$) is 11.4 ppm that is slightly larger than that of Möbius aromatic conformer of free-base [28]hexaphyrin (10.2 ppm). The HOMA and NICS values also represent the Möbius aromaticity of **2** (0.61 and -14.9 ppm)

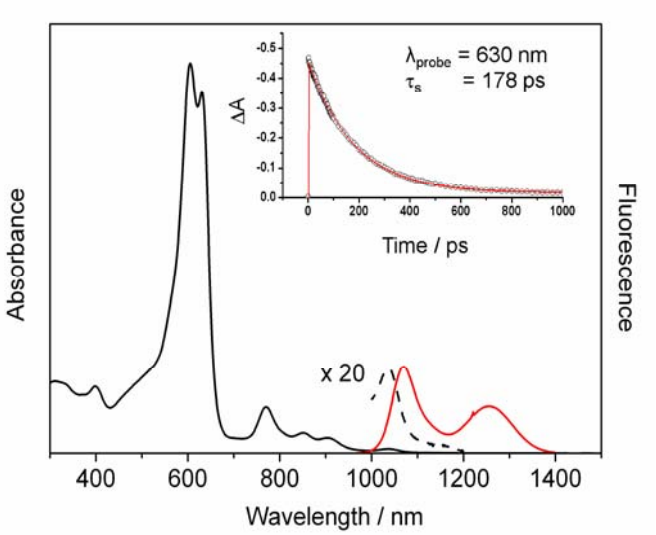

Fig. 3 Steady-state absorption (black line) and fluorescence (red line) and femtosecond transient absorption decay profile (inset) of **2**.

The steady-state absorption spectrum of **2** exhibits the split B-like band and well-resolved Q-like bands, reflecting its aromatic character (**Fig. 3**). According to the TD-DFT calculations, the split B-like band arises from its electronic transition nature, not from the presence of other conformers. Unlike **1**, **2** shows the structured fluorescence spectrum with a vibronic band, and its singlet excited-state lifetime is estimated to be 178 ps by a single exponential decay function (**Fig. 4**). Considering these two aspects, **2** is conformationally locked into a stable Möbius structure with better structural rigidity despite its twisted topology. The TPA cross-section value of **2** (8100 GM) also can be ranked high as compared with those of **1** and metal coordinated hexaphyrins, which strongly supports our conjecture that **2** steadily holds a stable Möbius topology with a nice π-conjugation network (**Fig.3**). In fact, the largest dihedral angle in the π-conjugation pathway of **2** (26.5°) is smaller than those of **1** (36°) and metalated hexaphyrins (46.5°). In this sense, the dihedral angle control, thus p-orbital overlap angle control between pyrroles, seems to be a key factor for realizing the Möbius aromatic expanded porphyrins. In the studies of ring-fused hexaphyrins, it should be noted that their singlet excited-state lifetimes are not short in view of their twisted topologies. Aromatic **2** presumed to be more rigid than ring-fused hexaphyrins shows much shorter singlet excited-state lifetime. This implies that the excited-state dynamics of expanded porphyrins is associated with not only molecular structure but aromatic character.

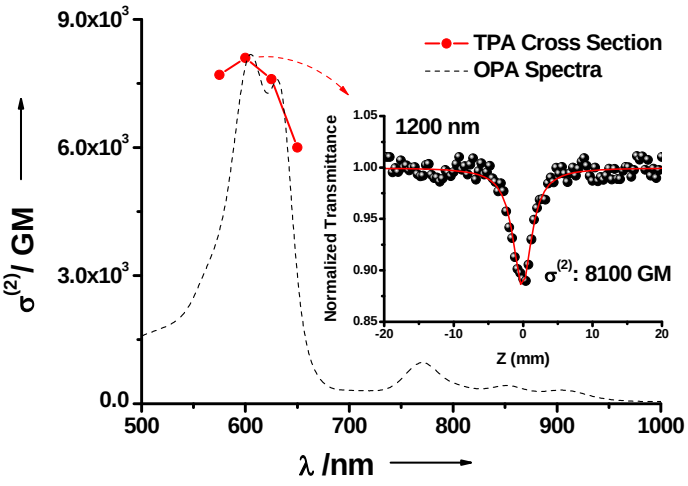

Fig. 4 TPA spectra of **2** in toluene. Inset show a Z-scan curve trace and best fitting curve at 1200 nm.

(2) Realization of Möbius aromatic molecule through protonation

The expanded porphyrins with [4*n*+2]π-electrons transform their conformations into planar topologies, whereas in the expanded porphyrins with [4*n*] π-electrons their conformations are changed to twisted Möbius strip-like topologies. This is very intriguing aspect because all these expanded porphyrins regardless of [4*n*+2] and [4*n*] π-electrons have twisted initial structures. One might expect that aromatic stabilization effect governs this different transformation that depends on the number of π-electrons, [4*n*+2] or [4*n*], during the protonation processes. However, we cannot confidently assert whether only aromatic stability leads to this result because protonated expanded porphyrins described above have different number of pyrrole units and *meso*-substituents as well as different number of π-electrons between [4*n*+2] and [4*n*] molecular groups. In this context, a recent study on the protonation of [36] and [38]octaphyrins with the same number of substituents can provide some evidences on this issue.[46] Also, in the former study about the Möbius aromaticity of protonated [32]heptaphyrins since their detailed spectroscopic analyses such as the fluorescence and excited-state dynamics have not been carried out, the protonation effects on the photophysical properties of [4*n*] expanded porphyrins can be deduced from this study.

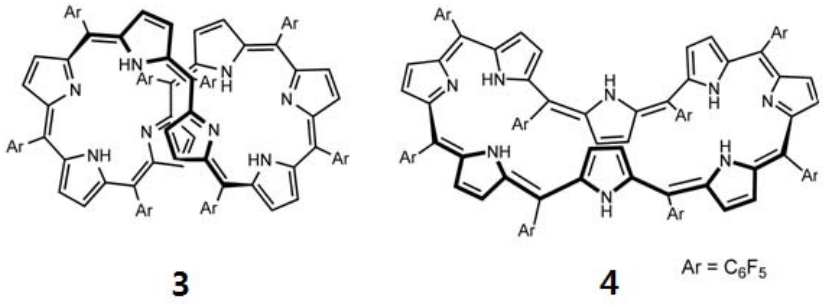

Chart3. Molecular structures [36]Octaphyrin **3** and [38]octaphyrin **4**.

① Photophysical Properties of Neutral [36]/[38] Octaphyrin

The neutral species of *meso*-octakis(pentafluorophenyl) [36] and [38] octaphyrins are considered to have different conformations each other (**Chart 3**). [36]Octaphyrin **3** shows twisted figure-of-eight topology in the X-ray crystallographic analysis and its ^{1}H NMR spectra indicate nonaromaric character with the signals of β-protons in 6 – 8 ppm region. On

the other hand, the X-ray crystal structure of [38]octaphyrin **4** could not be determined due to the lack of suitable single crystal, but less planar and symmetric conformation was suggested on the basis of its ^{1}H NMR spectra with moderate diatropic ring currents and clearly observed eight signals of sixteen β-protons. In consistent with its nonaromatic character, broad B-like bands appear in the steady-state absorption spectrum of **3** without distinct Q-like bands. However, the absorption spectrum of **4** exhibits the aromatic-like features showing B- and Q-like bands (**Fig. 5**).

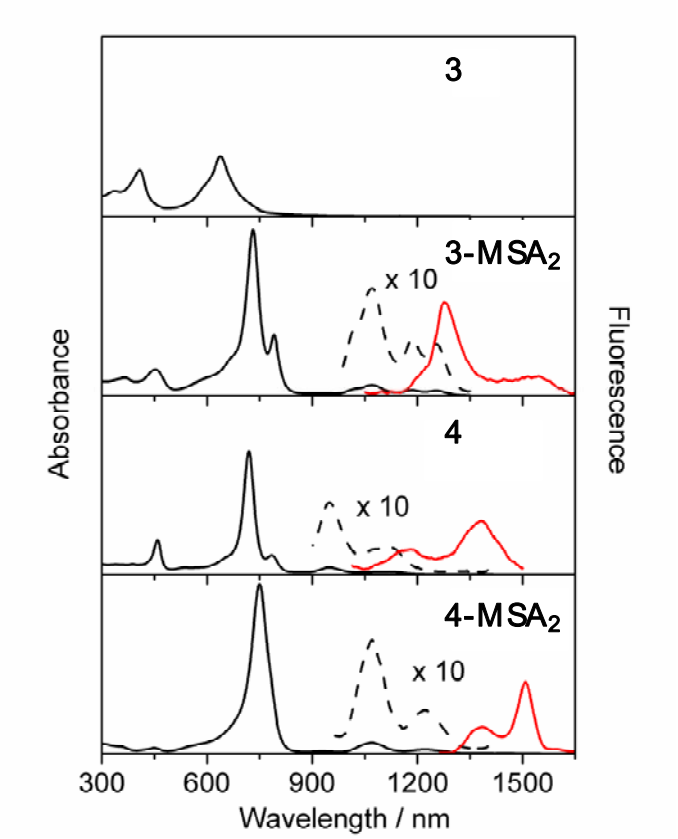

Fig. 5 Steady-state absorption (black line) and fluorescence (red line) spectra of neutral and protonated **3** and **4** in CH_2Cl_2.

② Aromaticity and Photophysical Properties of Protonated [36]/[38] Octaphyrin

Upon protonation, the conformations of both **3** and **4** are changed to even more extended topologies. Notably, diprotonated forms of **3** and **4** (**3-MSA**$_2$ and **4-MSA**$_2$, respectively) take macro-triangular shaped structures which are very similar to each other, evidenced by the X-ray crystallography. Only difference between the two structures is the

direction of two pyrroles in the molecules. In the structure of protonated form of **3**, these two pyrroles are significantly tilted with respect to the molecular plane defined by the rest of pyrrole units, which leads to twisted Möbius topology. On the contrary, all the pyrrole units in protonated form of **4** maintain nearly parallel direction to the molecular plane, which results in planar Hückel topology. Through detailed ^{1}H NMR experiments with varying temperature and addition amount of acids, it was also proved that the extent of aromaticity of two diprotonated forms becomes even stronger than that of neutral forms. In line with this, the absorption spectra of both diprotonated forms, show well-defined B- and Q-like bands indicating their strong aromatic characters (**Fig. 5**). Also, the fluorescence spectrum of protonated form of **3** was observed in contrast to the non-fluorescent behavior of its neutral form. Both neutral and protonated forms of **4** are fluorescent but the Stokes shift of protonated form is smaller than that of neutral form.

This fluorescence feature implies that molecular frameworks become more rigid by protonation regardless of their number of π-electrons. The excited-state dynamics of molecules strongly supports the enhancement of molecular rigidity in protonated forms. The singlet excited-state lifetimes of **3** and **4** are estimated to be 8.6 and 12.1 ps, respectively. After the protonation, however, the lifetimes increase to 32.1 and 40.7 ps, respectively. The triplet excited-state lifetimes also follow the trend in the singlet excited-state lifetimes. As mentioned before, flexible molecular framework stimulates the energy relaxation processes by providing efficient nonradiative decay pathways such as internal conversion. Therefore, the shorter excited-state lifetimes of neutral forms can be attributed to their structural flexibilities. In fact, the singlet excited-state lifetime of **3** shows probe wavelength dependence presumably due to the conformational heterogeneities, corroborating our interpretation. Inversely, the rigid molecular conformations induced by protonation lead to the longer excited-state lifetimes of protonated forms by impeding nonradiative decay pathways. Here, it should be noted that protonated form of **3** having twisted Möbius topology also shows increased singlet excited-state lifetime. In particular, it exhibits the longest triplet excited-state lifetime. This provides us with indirect evidences on aromatic stabilization effects which gives a stable conformation with twisted Möbius topology. The TPA cross-section values also support this inference. The neutral forms of **3** and **4** exhibit smaller TPA values compared to their protonated forms, and the largest value was observed for the protonated form of **3** in accordance with the triplet excited-state lifetimes.

Through this study, we have witnessed that by protonation the conformation of expanded

porphyrins is transformed to proper topology that makes their aromaticity increase regardless of the initial structures and the size of molecule. Thus [4n] expanded porphyrins take twisted Möbius topology and [4n+2] expanded porphyrins take planar Hückel topology. We do not know precisely what happens and how the conformations are changed in protonation processes, but we can imagine probable situations. In neutral conditions, intramolecular hydrogen bonding is strong enough to prevent from conforming to intrinsic aromaticity. However, under modest acidic conditions intramolecular hydrogen bonding is broken by protonation of iminic pyrrole and intermolecular hydrogen bonding between macrocycle, counter-anions, and acid molecules. Then, intrinsic aromaticity begins to govern the molecular conformation. After the transformations of topologies, they respectively accommodate themselves to stable conformations and environments, leading to longer lived excited state and enlarged TPA cross-section values. In this regard, it can be concluded that aromatic stabilization effect plays a major role in protonation-triggered conformational changes of expanded porphyrins although its extent of participation is still questionable.

(3) Realization of Möbius antiaromatic molecule through phosphorus coordination

Next, we have characterized the mono-phosphorus complexes of [28]hexaphyrins **5** and bis-phosphorus complexes **6** of [30]hexaphyrins as [4n]π Möbius aromatic and [4n+2]π Möbius antiaromatic compounds, respectively (**Chart 4**)

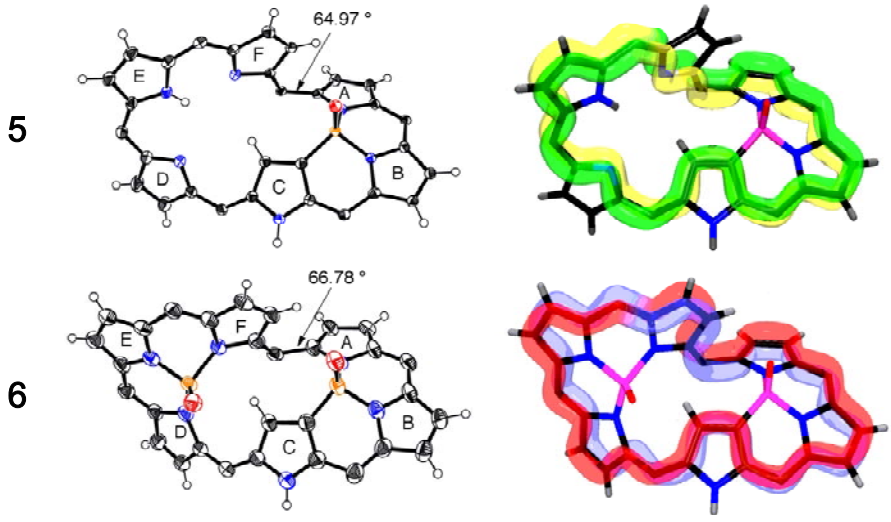

Chart4. X-ray crystal structures and schematic π-electron conjugation pathways of

mono-phosphorus **5** and Bis [28]hexaphyrins **6**.

① Aromaticity and photophysical properties of phosphorus coordinated hexaphyrins

Single-crystal X-ray diffraction analysis revealed a twisted Möbius structure of **5**, in which a P=O moiety was bound to the *β*-carbon atom of the pyrrole unit **C** and the two nitrogen atoms of the pyrrole units **A** and **B**. The ^{1}H NMR spectrum showed ten signals due to the outer *β*-protons in the range of 7.75–6.53 ppm and a doublet at δ = 2.99 ppm due to the inner *β*-proton of the pyrrole unit **C** that was coupled with ^{31}P with J = 6.9 Hz. Accordingly, the difference ($\Delta\delta$) between the chemical shifts of the most shielded and deshielded *β*-protons was 4.76 ppm, indicating a moderate diatropic ring current despite the largest dihedral angle (65°) along its π-conjugation. Accordingly, **5** has been assigned as a normal Möbius aromatic molecule.

The structure of bis-phosphorus complex **6** was unambiguously determined by X-ray diffraction analysis to be a singly twisted Möbius conformation, in which the additionally embedded P=O moiety was bound to the three nitrogen atoms of the pyrrole units **D**, **E**, and **F**. Interestingly, the ^{1}H NMR spectrum of **6** revealed a remarkably deshielded doublet at δ = 11.14 ppm due to the inner *β*-proton of the pyrrole unit **C** that was coupled with ^{31}P[a] (J = 5.0 Hz), ten signals due to the outer *β*-protons in a range of 6.72–5.54 ppm, and a relatively shielded broad singlet at δ = 7.15 ppm due to the outer NH proton. The observed apparent deshielding of the inner *β*-proton and significant shielding of the outer *β*-protons indicated a distinct paratropic ring current with $\Delta\delta$ = 5.60 ppm. The observed moderate ring current may be ascribed to a large dihedral angle (66.8°) at the most distorted position. The ^{1}H NMR analysis also indicated a moderate but distinct 30π-Möbius antiaromaticity of **6**. The most intriguing point here is that the shielding/deshielding effects of **5** and **6** are inverted only by changing the number of π-electrons from [4n] to [4n+2] though their Möbius-type structures remain nearly the same. This intimates to us that the concept of Möbius aromaticity, a reversal of Hückel rule, is fairly validated in the expanded porphyrin systems.

The UV/Vis/NIR absorption spectrum of **5** exhibits an intense B-like band at 588 nm and broad Q-like bands at 876 and 1055 nm, reveal porphyrin-like structure. The DFT calculation of **5** shows nearly degenerated HOMO and HOMO-1, being in accordance with its absorption spectrum. Moreover, **5** exhibits the fluorescence band at 1090 nm as a mirror image to the corresponding absorption spectrum. In contrast, the UV/Vis/NIR absorption spectrum of **6** shows ill-defined Soret-like bands and smeared NIR bands, without fluorescence emission. It should be noted that these absorption and fluorescence behaviors of **6** are similar to those of typical Hückel antiaromatic expanded porphyrins.

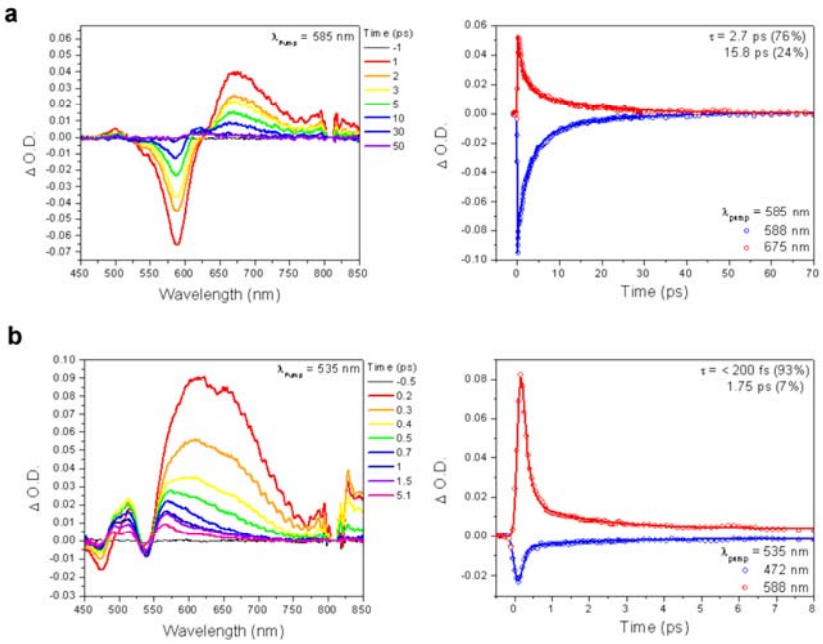

Fig. 6 Femtosecond transient absorption spectra and decay profiles. a: The pump excitation is 585 nm for **5**. b: The pump excitation is 535 nm for **6**.

Especially, the aromaticity of expanded porphyrin is prominently distinguished in time-resolved and non-linear optical (NLO) spectroscopic measurements. The Möbius aromatic molecule, **5**, reveals the distinct excited-state properties of aromatic expanded porphyrins. Typically, we have observed that the differential absorption spectra show strong ground state bleaching (GSB) signals with relatively weak excited state absorption (ESA) signals in aromatic expanded porphyrins, which are also seen in the transient absorption spectra of **5**. In contrast, the spectral shapes of **6** featured by the small GSB and large ESA signals are quite different from those of **5** (**Fig. 6**). This spectral feature is unique in Hückel antiaromatic expanded porphyrins, together with faster decay dynamics of **6** than **5** as shown in Fig. 5. The difference in the excited-state dynamics between aromatic and antiaromatic expanded porphyrins could be mainly attributed to the different electronic structures of these two classes of molecules. As a consequence, it perturbs the electronic transitions or states affecting the steady- and excited-state dynamics.

The two-photon absorption (TPA) cross-section values of phosphorous hexaphyrins also exemplify the difference in aromaticity. The aromatic **5** shows relatively large TPA cross-section value of 3950 GM than that of the antiaromatic **6**, 2400 GM, which is also consistent with the approximate proportionality between the degree of aromaticity and TPA values as demonstrated in the previous studies.

② Quantum mechanical calculations of phosphorus coordinated hexaphyrins

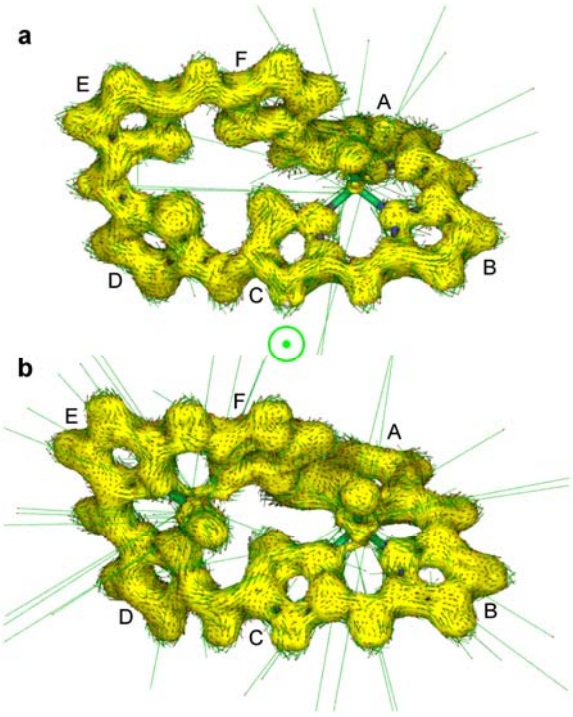

Fig. 7 a: The AICD plot for **5,**
b: The AICD plot for **6**

We performed quantum mechanical calculations (B3LYP/6-311G(d,p)) for **5** and **6** on the basis of the crystal and optimized structures. Large negative NICS values were calculated at the center of **5** (–8.25 ppm for the crystal structure and –11.99 ppm for the optimized structure) but small positive NICS values were calculated for **6** (+3.65 ppm for the crystal structure and +2.05 ppm for the optimized structure). In addition, we also attempted the direct visualization of induced ring current. Especially for nonplanar π-conjugated systems like **5** and **6**, AICD method is a powerful tool of determining the degree of aromaticity/antiaromaticity, because it represents the 3-dimensional image of delocalized electron densities with a scalar field. Since the AICD plot illustrates the paramagnetic term of the induced current density, the aromatic molecules show clockwise current density and the antiaromatic species show counter-clockwise. As shown in **Fig. 7**, the AICD plot of **5** reveals clear clockwise current density vectors, indicating a diamagnetic ring current. On the contrary, the AICD plot of **6** shows relatively weak counter-clockwise current flow, which means the induced paratropic ring current. Furthermore, the AICD plots of **5** and **6** show a prominent difference upon changing the isosurface values. While **5** reveals continuous boundary surface enclosing the delocalized electrons even at the isosurface value of 0.05, **6** does not show a continuous current density above the isosurface value of 0.045. This difference between **5** and **6** indicates that π-electron conjugation is more facile in **5** with [28] π-electronic distorted Möbius topology compared with **6** with [30] π-electronic circuit. These results demonstrate that **5** exhibits Möbius aromatic character with continuous and diamagnetic current density in its distorted conformation and that, more importantly, the Möbius antiaromaticity of **6** is revealed by 3-dimensional paratropic ring current in spite of a weak density of delocalized electrons.

In summary, the mono-phosphorus complexes of [28]hexaphyrins and bis-phosphorus complexes of [30]hexaphyrins have been synthesized and characterized as [4n]π Möbius aromatic and [4n+2]π Möbius antiaromatic compounds. The twisted Möbius structures are revealed by the single-crystal X-ray diffraction analysis. The aromaticity/antiaromaticity is measured according to the magnetic criteria and the photophysical properties. As a result, bis-phosphorus [30]hexaphyrins have been determined to be the first structually-characterized Möbius antiaromatic system, which is stable, neutral, and rigid.

5. Summary

Based on the spectroscopic techniques and theoretical approaches, the Möbius (anti)aromaticity in expanded porphyrins could be assigned. As illustrated in the above examples, it seems relatively easy to find out expanded porphyrins with [4n] π-electronic circuitry which exhibit Möbius topology, but it still remains as a challenge to recognize or characterize them. Nevertheless, the difficulties in realizing Möbius aromatic structures in [4n]annulens rely on the fact that the molecular twisting towards Möbius structures only requires shallow energy barriers, resulting in an easy flipping back to Hückel topology. Thus, "the locking into a Möbius structure" in [4n] annulenes is hardly achieved. But in expanded porphyrins, there are some definite advantages in the formation of Möbius aromatic molecules like (i) overall conformational flexibility, (ii) an ability to invert, or "flip out" the constitutional pyrrolic subunits under certain conditions, (iii) the capacity to respond to two-electron reduction and oxidation through the facile release or capture of a pair of pyrrolic NH hydrogen atoms thus balancing charge and (iv) the possibility of "locking in" twisted conformations through metalation, especially in those cases that permit the formation of both N—metal and C—metal bonds.

Based on this project, we demonstrate that the distorted molecular conformations of expanded porphyrins, which are unavoidable especially as the number of pyrrole rings increases, can be controlled, leading to the planar structures to increase the aromaticity determined by Hückel's [4n + 2] rule. In conclusion, the synthetic methods of Möbius (anti)aromatic expanded porphyrins are now in actively progress. In line with exploring their interesting π-electronic properties, many new research areas in Möbius (anti)aromatic expanded porphyrins will be widely open in the near future.

6. References

(1) J. L. Sessler, A. Gebauer and S. J. Weghorn, *The Porphyrin Handbook*, K. M. Kadish, K. M. Smith and R. Guilard, Academic Press, New York, 2000, vol. 2, ch. 9, pp. 55–124.

(2) J. M. Lim, Z. S. Yoon, J.-Y. Shin, K. S. Kim, M.-C. Yoon, D. Kim, *Chem. Commun.,* 2009. 261.

(3) J. L. Sessler and S. J. Weghorn, Expanded Contracted and Isomeric Porphyrins, ed. J. E. Baldwin, Pergamon, New York, 1997.

(4) T. K. Chandrashekar, S. Venkatraman, *Acc. Chem. Res.,* 2003, ***36***, 676.

(5) M. K. Cyranski, *Chem. Rev.,* 2005, ***105***, 3773.

(6) S. Mori, K. S. Kim, Z. S. Yoon, S. B. Noh, D. Kim, A. Osuka *J. Am. Chem. Soc.,* 2007, ***129***, 11344.

(7) J. L. Sessler and D. Seidel, *Angew. Chem., Int. Ed.,* 2003, ***42***, 5134.

(8) Z. S. Yoon, J. H. Kwon, M.-C. Yoon, M. K. Koh, S. B. Noh, J. L. Sessler, J. T. Lee, D. Seidel, A. Aguilar, S. Shimizu, M. Suzuki, A. Osuka and D. Kim, *J. Am. Chem. Soc.,* 2006, ***128***, 14128.

(9) H. Lee, S. -Y. An, M. Cho, *J. Phys. Chem. B,* 1999, ***103***, 4992.

(10) F. Meyers, S. R. Marder, B. M. Pierce, J. L. Brédas, *J. Am. Chem. Soc.,* 1994, **116**, 10703.

(11) J. Juselius, D. Sundholm, *Phys. Chem. Chem. Phys.,* 2000, ***2***, 2145.

(12) M.-C. Yoon, S. Cho, M. Suzuki, A. Osuka, D. Kim *J. Am. Chem. Soc.,* 2009, **131**, 7360

(13) R. Herges, *Chem. Rev.,* 2006, ***106***, 4820.

(14) E. Heilbronner, *Tetrahedron Lett.,* 1964, **5**, 1923.

(15) D. Ajami, O. Oeckler, A. Simon, R. Herges, *Nature,* 2003, **426**, 819.

(16) C. Castro, Z. Chen, C. S. Wannere, H. Jiao, W. L. Karney, M. Mauksch, R. Puchta, N. J. R. v. E. Hommes, P. v. R. Schleyer, *J. Am. Chem. Soc.,* 2005, ***127***, 2425.

(17) J. L. Sessler, S. J. Weghorn, V. Lynch, M. R. Johnson, *Angew. Chem., Int. Ed.,* 1994, ***33***, 1509.

(18) Z. S. Yoon, A. Osuka, D. Kim, *Nature Chem.,* 2009, ***1***, 113.

(19) M. Stępień, L. Latos-Grażyński, N. Sprutta, P. Chwalisz, L. Szterenberg, *Angew. Chem., Int. Ed.,* 2007, ***46***, 7869.

(20) R. Herges, *Nature,* 2007, ***450***, 36.

(21) E. Pacholska-Dudziak, J. Skonieczny, M. Pawlicki, L. Szterenberg, Z. Ciunik, L. Latos-Grażyński , *J. Am. Chem. Soc.,* 2008, ***130***, 6182.

(22) Y. Tanaka, S. Saito, S. Mori, N. Aratani, H. Shinokubo, N. Shibata, Y. Higuchi, Z. S. Yoon, K. S. Kim, S. B. Noh, J. K. Park, D. Kim, A. Osuka, *Angew. Chem., Int. Ed.,* 2008, ***47***, 681 and references therein.

(22) K. S. Kim, Z. S. Yoon, A. B. Ricks, J.-Y. Shin, S. Mori, J. Sankar, S. Saito, Y. M. Jung, M. R. Wasielewski, A. Osuka, D. Kim, *J. Phys. Chem. A*, 2009, ***113***, 4498.

(23) J.-Y. Shin, J. M. Lim, Z. S. Yoon, K. S. Kim, M.-C. Yoon, S. Hiroto, H. Shinokubo, S. Shimizu, A. Osuka, D. Kim, *J. Phys. Chem. B*, 2009, ***113***, 5794.

(24) S. Tokuji, J.-Y. Shin, K. S. Kim, J. M. Lim, K. Youfu, S. Saito, D. Kim, A. Osuka, *J. Am. Chem. Soc.*, 2009, ***131***, 7240.

7. List of Publications

1. Meso-β Doubly Linked Zn(II) Porphyrin Trimers : Distinct anti-versus-syn Effects on Their Photophysical Properties
Toshiaki Ikeda, Naoki Aratani, Shanmugam Easwaramoorthi, Dongho Kim, Atsuhiro Osuka
Orgarnic Letters, **2009**, *11(14)*, 3080–3083

2. Regioselective Ru-Catalyzed Direct 2,5,8,11-Alkylation of Perylene Bisimides
Satomi Nakazono, Yusuke Imazaki, Hyejin Yoo, Jaesung Yang, Takahiro Sasamori, Norihiro Tokitoh, Tassel C_dric, Hiroshi Kageyama, Dongho Kim, Hiroshi Shinokubo, Atsuhiro Osuka
Chemistry-A European Journal, **2009**, *15(31)*, 7530–7533

3. Thermal Fusion Reactions of meso-(3-Thienyl) Groups in [26] Hexaphyrins to Produce Möbius Aromatic Molecules
Mitsunori Inoue, Kil Suk Kim, Masaaki Suzuki, Jong Min Lim, Jae-Yoon Shin, Dongho Kim, Atsuhiro Osuka
Angewandte Chemie International Edition, **2009**, *48(36)*, 6687–6690

4. Structural Factors Determining Photophysical Properties of Directly Linked Zinc(II) Porphyrin Dimers: Linking Position, Dihedral Angle, and Linkage Length
Sung Cho, Min-Chul Yoon, Jong Min Lim, Pyosang Kim, Naoki Aratani, Yasuyuki Nakamura, Toshiaki Ikeda, Atsuhiro Osuka, Dongho Kim
Journal of Physical Chemistry B **2009**, *113(31),* 10619–10627

5. Versatile Photophysical Properties of meso-Aryl-Substituted Subporphyrins: Dipolar and Octupolar Charge-Transfer Interactions
Shanmugam Easwaramoorthi, Jae-Yoon Shin, Sung Cho, Pyosang Kim, Yasuhide Inokuma, Eiji Tsurumaki, Atsuhiro Osuka, Dongho Kim
Chemistry-A European Journal, **2009**, *15(44)*, 12005–12017

6. Structural Dependence on Excitation Energy Migration Processes in Artificial Light

Harvesting Cyclic Zinc(II) Porphyrin Arrays
Min-Chul Yoon, Sung Cho, Pyosang Kim, Takaaki Hori, Naoki Aratani,Atsuhiro Osuka, Dongho Kim
Journal of Physical Chemistry B **2009**, *113(45),* 15074–15082

7. Synthesis of Arylated Perylene Bisimides through C–H Bond Cleavage under Ruthenium Catalysis
Satomi Nakazono, Shanmugam Easwaramoorthi, Dongho Kim, Hiroshi Shinokubo, Atsuhiro Osuka
Orgarnic Letters, **2009**, *11* (23), 5426–5429

8. Doubly β-Functionalized Meso-Meso Directly Linked Porphyrin Dimer Sensitizers for Photovoltaics
Jong Kang Park, Jinping Chen, Hye Ryun Lee, Sun Woo Park, Hiroshi Shinokubo, Atsuhiro Osuka, Dongho Kim
Journal of Physical Chemistry C, **2009**, *113* (52), 21956–21963

9. Meso-Trialkyl-Substituted Subporphyrins
Shin-ya Hayashi, Yasuhide Inokuma, Shanmugam Easwaramoorthi, Kil Suk Kim, Dongho Kim, Atsuhiro Osuka
Angewandte Chemie International Edition, **2010**, *49*(2), 321–324

10. Fluorescence Dynamics of Chlorophyll Trefoils in the Solid State Studied by Single-Molecule Fluorescence Spectroscopy
Ji-Eun Lee, Jaesung Yang, Victoria L. Gunderson, Michael R. Wasielewski, Dongho Kim
The Journal of Physical Chemistry Letters. **2010**, *1(1)*, 284–289

11. Comparative Spectroscopic Studies on Porphyrin Derivatives: Electronic Perturbation of N-confused and N-fused porphyrins
Jae Seok Lee, Jong Min Lim, Motoki Toganoh, Hiroyuki Furuta, Dongho Kim
Chemical Communications, **2010**, *46(2)*, 285–287

12. Protonated [4n]π and [4n+2]π Octaphyrins Choose Their Möbius/Hückel Aromatic Topology
Jong Min Lim, Jae-Yoon Shin, Yasuo Tanaka, Shohei Saito, Atsuhiro Osuka, Dongho Kim
Journal of the American Chemical Society , **2010**, *132*(9), 3105–3114

13. Defining Spectroscopic Features of Heteroannulenic Antiaromatic Porphyrinoids
Sung Cho, Zin Seok Yoon, Kil Suk Kim, Min-Chul Yoon, Dong-Gyu Cho, Jonathan L. Sessler, Dongho Kim
Journal of Physical Chemistry Letters, 2010, **2010**, *1* (6), 895–900

14. Excimer Formation Dynamics of Intramolecular π-Stacked Perylenediimides Probed by Single-Molecule Fluorescence Spectroscopy

Hyejin Yoo, Jaesung Yang, Andrew Yousef, Michael R. Wasielewski , Dongho Kim

Journal of the American Chemical Society, **2010**, *132* (11), 3939–3944

15. Large Porphyrin Squares from the Self-assembling of meso-Triazole-Appended L-shaped meso–meso Linked Zn(II) Triporphyrins: Synthesis and Efficient Energy Transfer

Chihiro Maeda , Pyosang Kim , Sung Cho , Jong Kang Park, Jong Min Lim , Dongho Kim, Josh Vura-Weis , Michael R. Wasielewski, Hiroshi Shinokubo, Atsuhiro Osuka,

Chemistry-A European Journal, **2010**, *16*(17), 5052–5061

16. A Stable Non-Kekulé Singlet Biradicaloid from *meso*-Free 5,10,20,25-Tetrakis(Pentafluorophenyl)-Substituted [26]Hexaphyrin(1.1.1.1.1.1)

Taro Koide, Ko Furukawa, Hiroshi Shinokubo, Jae-Yoon Shin, Kil Suk Kim, Dongho Kim, Atsuhiro Osuka,

Journal of the American Chemical Society, **2010**, *132* (21), 7246–7247

17. Photophysical Properties of N-Confused Hexaphyrins: Effects of Confusion of Pyrrole Rings and Molecular Shape on Electronic Structures

Jong Min Lim, Jae Seok Lee, Hyun Woo Chung, Hee Won Bahng, Keisuke Yamaguchi, Motoki Toganoh, Hiroyuki Furuta, Dongho Kim

Chemical Communications, **2010**, *46(24)*, 4357–4359

18. Möbius Antiaromatic Bisphosphorus Complexes of [30]Hexaphyrins

Tomohiro Higashino, Jong Min Lim, Takahiro Miura, Shohei Saito, Jae-Yoon Shin, Dongho Kim, Atsuhiro Osuka

Angewandte Chemie International Edition, **2010**, 49(29), 4950-4954

19. Aromaticity and Photophysical Properties of Various Topology-Controlled Expanded Porphyrins

Jae-Yoon Shin, Kil Suk Kim, Min-Chul Yoon, Jong Min Lim, Zin Seok Yoon, Dongho Kim, Atsuhiro Osuka

Chemical Society Reviews, **2010**, 39(8), 2751–2767

Attachment for Research Highlight

Möbius Aromaticity in Various Expanded Porphyrins

During the period for *AFSOR/AOARD project (**FA2386-09-1-4092**)*, Prof. Kim's group has collaborated with Prof. A. Osuka at the Kyoto University in order to find out the Möbius (anti)aromatic molecules and investigate their detailed natures by various spectroscopic methods. Finally, they have discovered many types of expanded porphyrins with Möbius topology and explored their interesting photophysical properties.

Nature Chemistry **(Review Article)** **(Year 2009, Vol. 1, Issue: 2, Page 113 – 122)**	
Selected as **Editor's Choice** **in Science** **(Year 2009, Vol. 324, Issue 5930, Page 990)**	
Selected as **Research Highlight in** **Chemical & Engineering News** **(Year 2009, Vol. 87, Issue 21, Page 35)**	

DD882: As a separate document, please complete and sign the inventions disclosure form.

This document may be as long or as short as needed to give a fair account of the work performed during the period of performance. There will be variations depending on the scope of the work. As such, there are no length or formatting constraints for the final report. Include as many charts and figures as required to explain the work. A final report submission very similar to a full length journal article will be sufficient in most cases.